

光学学报

矢量涡旋光束的生成与模式识别方法

付时尧^{1,2,3*}, 高春清^{1,2,3**}

¹北京理工大学光电学院, 北京 100081;

²信息光子技术工业和信息化部重点实验室, 北京 100081;

³光电成像技术与系统教育部重点实验室, 北京 100081

摘要 与宏观物体类似, 光子等微观粒子也可携带角动量。光子的角动量包括自旋角动量和轨道角动量, 两种角动量的共同作用产生了一种新型结构光束, 即矢量涡旋光束。矢量涡旋光束具有各向异性的波面和偏振分布, 提供了多种光场自由度, 在量子技术、光通信、激光探测、激光加工、高分辨成像、光镊等前沿领域展现了巨大的应用潜力, 吸引了国内外学者的广泛关注。高效地生成矢量涡旋光束, 以及高精度地识别矢量涡旋光束的模式分布, 是其应用的关键。本文简要回顾了国内外学者在矢量涡旋光束的生成与模式识别方面的研究工作, 同时系统梳理了本文作者过去十年在该方面的研究进展, 重点介绍了其相关代表性成果。

关键词 物理光学; 激光光场调控; 矢量涡旋光束; 轨道角动量; 自旋角动量

中图分类号 O436

文献标志码 A

DOI: 10.3788/AOS230651

1 引言

角动量是描述物体旋转运动的物理量, 从宏观物体到光子等微观粒子均可携带角动量。早在 1909 年, 坡印廷就已经预测圆偏振光携带有角动量^[1], 1936 年 Beth 等^[2]首次通过石英细丝悬挂半波片的方式观测到了光束的自旋角动量(SAM), 且光束的 SAM 只有两个本征值 ± 1 , 分别对应左右旋圆偏振态, 每一个光子携带的 SAM 值为 $\pm \hbar$ 或 $-\hbar$ (\hbar 为约化普朗克常量)。1950 年, 研究人员发现电多级辐射过程将产生携带轨道角动量(OAM)的电磁辐射^[3], 预测了光束也可携带 OAM。1992 年, Allen 等^[4]证明了具有螺旋波前 $\exp(i l \varphi)$ 的光束携带 OAM(l 为拓扑荷数, 也称为角量子数, 可为任意整数, φ 为角向坐标), 且该光束中的每一个光子携带的 OAM 值为约化普朗克常量 \hbar 的整数倍 $l\hbar$ 。至此, 彻底开启了有关光束角动量研究的大门^[5]。

携带 OAM 是具有螺旋波前光束的固有属性, 通过对光束 OAM 自由度的调控可以获得不同阶次的 OAM 光束, 这种光束与平面波干涉时, 其干涉场呈现涡旋状强度分布, 因此也被称为涡旋光束^[6]。当协同调控 SAM 与 OAM 的自由度时, 则可以获得具有横截

面各向异性偏振分布的矢量涡旋光束^[7-8], 这种光束兼具相位涡旋与偏振涡旋特性, 是涡旋光束的一种广义形式, 已被证明在激光通信^[9-13]、旋转探测^[14-18]、光镊^[19-20]、量子技术^[21-23]、激光加工^[24-26]、高分辨率成像^[27]等领域具有广阔的应用前景。

针对不同应用场景, 所需的矢量涡旋光束的模式阶次、模场分布不尽相同, 由此对矢量涡旋光束的生成及模式感知提出了更高要求。因此, 矢量涡旋光束的高效按需生成及高精度模式识别是其上述应用的重中之重, 直接决定了应用系统的性能。本文总结了近几年矢量涡旋光束的生成及模式识别的主要方法, 在简要回顾国内外学者的研究进展的基础上, 重点介绍了本文作者团队在该领域的代表性研究工作。本文将从矢量涡旋光束的基本性质、生成技术与模式识别技术分块展开。

2 矢量涡旋光束的基本原理

矢量涡旋光束 $|\Psi\rangle$ 可表示为旋向相反的携带不同 OAM 的圆偏振光束的同轴叠加:

$$|\Psi\rangle = |\Psi_R^m\rangle |R_m\rangle + |\Psi_L^l\rangle |L_l\rangle \quad (1)$$

式中, $|R_m\rangle$ 和 $|L_l\rangle$ 可表示为

$$|R_m\rangle = \exp(im\varphi)[1, i]^T / \sqrt{2}, \quad (2)$$

收稿日期: 2023-03-08; 修回日期: 2023-03-23; 录用日期: 2023-04-03; 网络首发日期: 2023-04-13

基金项目: 国家重点研发计划(2022YFB3607700)、国家自然科学基金(11834001, 61905012)、国防基础科研计划(JCKY2020602C007)、北京市自然科学基金(1232031)、中央高校基本科研业务费专项资金(2022CX11006)、教育部基金(8091B042109)

通信作者: *fushiyao@bit.edu.cn; **gao@bit.edu.cn

$$|L_l\rangle = \exp(i\varphi)[1, -i]^T/\sqrt{2}, \quad (3)$$

式中, Ψ_R^m 和 Ψ_L^l 为复系数, 表征了圆偏振分量 $|R_m\rangle$ 和 $|L_l\rangle$ 的振幅和初始相位; l 和 m 分别为左、右旋涡旋光束的拓扑荷数。由于宏观上的圆偏振态对应微观上光子的自旋角动量, 因此矢量涡旋光束也可理解为由一系列具有相反 SAM 且携带不同 OAM 的光子叠加而成。另一方面, 如果用 $|L\rangle$ 和 $|R\rangle$ 分别表示左、右旋圆偏振态, $|l\rangle$ 和 $|m\rangle$ 分别表示拓扑荷数为 l 和 m 的 OAM 态, 则式(1)还可表示为

$$|\Psi\rangle = \alpha|L\rangle|l\rangle + \beta|R\rangle|m\rangle, \quad (4)$$

式中, α, β 为复系数。式(4)表明矢量涡旋光束可表示为 SAM 与 OAM 的直积态叠加, 形成与量子纠缠 Bell 态表达形式类似的经典不可分离态^[28-30], 因此也有文献称矢量涡旋光束为一种“经典纠缠”光束^[31-33]。根据前述分析不难看出, 矢量涡旋光束本质上是对光场 OAM 与 SAM 双自由度协同调控的结果, 事实上, 通过对 OAM 及其他光场自由度的协同调控还可获得如 OAM 光梳^[34]、时空涡旋^[35-37]、光涡环^[38]、高维涡旋阵列^[39-43]、SU(2)几何模式光束^[44-46]等新型结构光场。

完备的表征矢量涡旋光束的模场分布对于研究其模场特性、生成与模式识别技术等至关重要。由于矢量涡旋光束是 SAM 和 OAM 联合调控下的结果, 因此可以直接用式(4)给出的 SAM 与 OAM 的直积态求和来表征。此外, 为了实现更直观的表征, 研究人员从斯托克斯矢量及庞加莱球模型^[47]出发, 依次提出了高阶斯托克斯矢量、高阶庞加莱球模型^[48-49], 以及杂合斯托克斯矢量和杂合庞加莱球模型^[50], 通过分析高阶/杂合斯托克斯矢量分布, 或分析模式所处的高阶/杂合庞加莱球球面位置来表征矢量涡旋光束。后来又进一步提出了广义庞加莱球模型, 将矢量涡旋模式的表征延伸至球内点, 用以表征偏振度小于 1 的各向异性偏振光束^[51]。这种以斯托克斯参量分布或庞加莱球表征矢量涡旋光束的方法直观且可靠, 可直接读出矢量涡旋光束的模场分布, 但在表征矢量涡旋光束的模场演化, 特别是从数学推导预测模场变化的角度来看还存在一定局限。

本文作者团队于 2021 年提出了一种矢量涡旋光束的四参量表征方法^[52], 该方法仍基于杂合庞加莱球模型, 但将杂合庞加莱球简化为四个参量 $\{m, l, \theta, \rho\}$, 其中 m 和 l 为矢量涡旋光束在圆偏正交基下分解得到的两个圆偏振分量的拓扑荷数[式(2)和式(3)], 定义了矢量涡旋光束所处的庞加莱球阶次; θ 和 ρ 则为矢量涡旋光束在庞加莱球球面位置的经纬坐标。不难看出, 通过 $\{m, l, \theta, \rho\}$ 即可确定矢量涡旋光束所处的庞加莱球阶次及球面位置, 进而完备表征矢量涡旋光束的模场分布。此外, 该表征方法的另一优点在于, 若将其写成向量形式 $[m, l, \theta, \rho]$, 则可构建推导得到不

同矢量涡旋模式间的变换矩阵, 这表明常见的光子 SAM 转化器件(如半波片等)、SAM-OAM 耦合器件(如 Q 波片等)均可用变换矩阵来表征。因此, 当一束矢量涡旋光束依次通过多个 SAM 转化器件、SAM-OAM 耦合器件时, 可通过变换矩阵求得出射光场的四参量表征, 进而预测出射矢量涡旋光束的模场分布^[52]。

3 矢量涡旋光束的生成方法

3.1 腔外模式转化

矢量涡旋光束的腔外模式转化生成, 即在激光谐振腔外将其他模场分布的光束(通常为基模高斯光束)转化成矢量涡旋光束。腔外模式转化法是最早提出的矢量涡旋光束生成方法之一, 也是当前最成熟的生成方法。从转化形式上来看, 可分为间接转化和直接转化两类。

间接转化可通过式(1)来理解。式(1)表明, 生成矢量涡旋光束的核心在于 OAM 调控, 即先通过一定技术手段将激光器产生的基模高斯光束转化为 OAM 光束, 而后通过偏振合成两束不同拓扑荷数的 OAM 光束来间接获得矢量涡旋光束。在这一思路下, 国内外学者开展了大量的研究工作, 提出了一系列矢量涡旋光束的间接偏振合成方法, 比较有代表性的包括 Sagnac 干涉法^[53-55]、Rochi 光栅法^[56]、直角棱镜法^[57]等。本文作者团队也提出了泰曼格林干涉^[58]、类 Sagnac 干涉^[59-60]、渥拉斯通棱镜法^[61-62]等矢量涡旋光束生成技术, 其中, 基于渥拉斯通棱镜, 本文作者团队报道了一种可编程矢量涡旋光束生成技术^[62], 其基本结构如图 1 所示。该方法采用液晶空间光调制器编码全息光栅的方式, 实现对入射基模高斯光束的 OAM、波矢、振幅和初始平面相位四个自由度的协调调控, 进而在土 1 衍射级上同时生成两束不同的 OAM 光束, 而后通过半波片、1/4 波片、渥拉斯通棱镜等偏振转化合成矢量涡旋光束。这一生成系统的优势在于, 液晶空间光调制器上编码的全息光栅透过率函数可通过计算机控制, 进而实现了任意矢量涡旋光束的可编程生成^[62]。

前述腔外间接生成矢量涡旋光束方法均采用了搭建干涉系统非共路合成的方式, 对系统的稳定性要求较高。基于液晶空间光调制器的纯相位调制特性, 研究人员提出了矢量涡旋光束的共路合成方法^[63-66]。该方法的原理在于, 纯相位液晶空间光调制器只能纯相位调控某一线偏振态的入射光束, 而对另一正交偏振态的入射光束没有影响, 因此可通过单一液晶空间光调制器分屏或级联双调制器的方式分别调控入射光束正交偏振分量的 OAM 态, 以此一路上偏振合成矢量涡旋光束, 系统稳定性显著提高。在该思路下, 本文作者团队报道了完美矢量涡旋光束^[67]、矢量涡旋光束阵列^[40-41, 68]等一系列复杂结构光场的生成工作, 并进一步提出了任意偏振态分布复杂矢量涡旋光场的生成方

法^[69-70]。除了上述通过OAM光束偏振合成外,矢量涡旋光束还可通过厄米高斯光束偏振合成^[71-73],其原理

在于矢量涡旋光束可在厄米高斯光束的模式基底下分解,具体方法细节此处不再赘述。

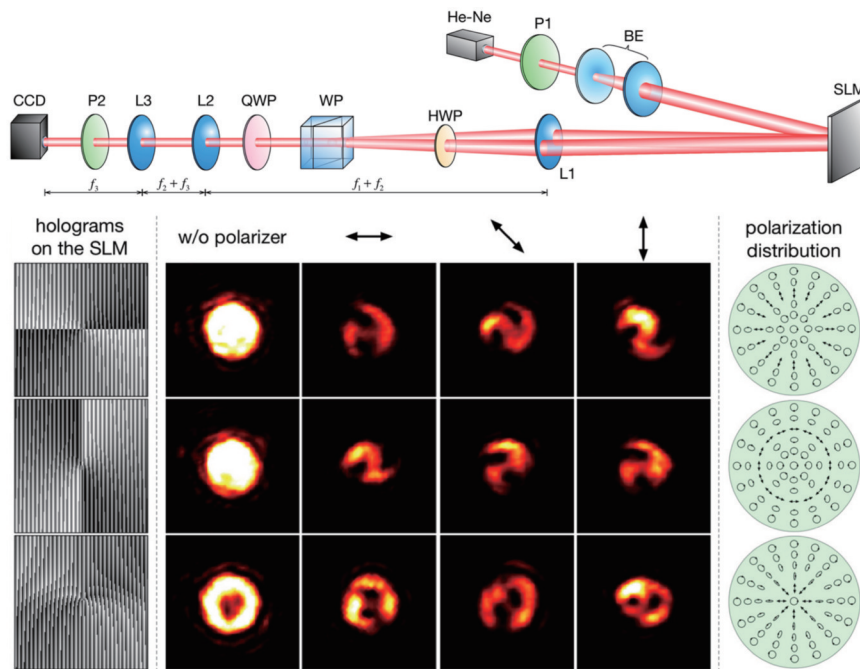


图1 可编程矢量涡旋光束的腔外生成方法^[62]

Fig. 1 Method for extracavity generation of programmable vector vortex beams^[62]

随着微纳加工技术的不断进步,相继报道了一系列基于光子自旋霍尔效应^[74-76]的新型光子SAM-OAM耦合器件,实现了由高斯光束至矢量涡旋光束的直接转化,可实现上述功能的代表性器件包括Q波片、组合半波片、超表面等。Q波片是一种各向异性主轴排布的几何相位调控器件^[77],一般采用液晶等双折射材料制成,以其小型化、轻量化等优势迅速成为腔外生成矢量涡旋光束的主要途径之一。Q波片生成矢量涡旋光束的原理在于,当圆偏振光入射时,出射光仍为圆偏振光,但其旋向相反,并被引入额外OAM。当入射的圆偏振光旋向相反时,其引入的OAM相反。由于线偏振光可看作两束旋向相反的圆偏振光的叠加,因此当线偏振光入射Q波片时,其输出光即可满足式(1),进而生成了矢量涡旋光束^[78]。此外,通过切割半波片并重新组合的方式构成离散结构的Q波片,即组合半波片,也可实现与Q波片类似的功能^[79]。超表面是一种二维亚波长阵列结构,具有较强的光场调控能力,通过优化超表面阵列天线的几何参数、排布角度等,可为入射光束引入理想的相位、偏振分布,进而生成矢量涡旋光束^[80-86]。

3.2 腔内模场调控

腔内模场调控方法是指通过一定技术手段使高阶矢量涡旋模式在激光谐振腔内直接振荡,实现激光器直接输出复杂矢量涡旋光束,相比于腔外模式转化方法具有系统稳定、输出模式纯度较高、利于集成化和工程化等优势,成为近几年光场调控领域的研究热点^[87]。

从矢量涡旋光束的产生机理上来看,腔内模场调控可主要分为两大类,第一类即设法抑制腔内基模振荡,以使高阶横模——拉盖尔高斯模式起振。采用环形泵浦的方式可有效改变谐振腔内的模式匹配方式,达到抑制基模的目的。例如,2015年,Kim等^[88]报道了采用808 nm环形光束泵浦Nd:YVO₄并配合标准具选模的方式生成±1阶涡旋光束。后来亦有采用环形泵浦微片等生成矢量涡旋光束的报道,但普遍模式阶次不高^[89-95]。与环形泵浦类似,若在谐振腔镜中心引入损耗点,也可达到抑制腔内基模振荡的目的。在这一思路下,2018年,Qiao等^[96]通过在输出镜上刻蚀孔径,利用模式损耗对激光横模进行调控,获得高达288阶的OAM光束的输出,创造了固体激光器输出的最高OAM阶次纪录,后来,同一团队又采用在谐振腔镜刻蚀同心损耗环的方式,获得了多个高阶OAM模式的同时振荡,并与腔内锁模技术相结合演示了涡旋光场的时空编码通信^[97]。将谐振腔镜换成液晶空间光调制器,则可以动态调控腔内损耗,实现包括矢量涡旋光束在内的高阶横模的“数字化”输出,构成了数字激光器,然而,由于液晶空间光调制器的损伤阈值较低,使得数字激光器不易输出高功率矢量涡旋光束^[98]。

第二类即在腔内置入模式转化器件,使腔内振荡模式往复转化,当满足基模-矢量涡旋模式自治条件时,即可形成稳定振荡,进而输出矢量涡旋光束。为了实现这一功能,2016年,Naidoo等^[99]在激光谐振腔内置入Q波片实现腔内光子SAM-OAM耦合,最终使激

光器直接输出了柱矢量光束,通过旋转腔内Q波片、1/4波片等方式还可按需调控出射光束的模场分布。后来,同一课题组又将采用超表面制成的J波片融合进来,使激光器直接输出矢量涡旋光束^[100]。此外,基于泰伯效应,还可在腔内置入超表面阵列,从而使激光器直接输出矢量涡旋光束阵列^[101]。合理地利用像差亦可实现腔内模式转化功能,2022年,Sheng等^[102]在激光谐振腔内置入一系列光学透镜引入球差,最终获得了OAM阶次达95阶的多环结构涡旋光束的输出。

本文作者团队亦在全固态矢量涡旋激光器方面开展了探索性工作,实现了腔内光场横纵模协同调控,并搭建了多种人眼安全波段矢量涡旋光束原理样机^[103-105],如图2所示。2019年,本文作者团队报道了一种矢量涡旋光束激光器,该激光器采用V形谐振腔

结构[图2(a)],以半导体激光泵浦Er:YAG晶体,在腔内置入液晶Q波片及1/4波片引入光子SAM-OAM耦合,获得了波长为1645 nm的高阶矢量涡旋光束输出^[103]。在该激光系统中,通过旋转Q波片及1/4波片即可改变输出矢量涡旋光束的模场分布。进一步地,还搭建了环形腔矢量涡旋光束激光器[图2(b)],其仍采用半导体激光泵浦Er:YAG晶体,通过腔内置入光隔离器实现振荡模式单向运转,有效地消除了增益介质的空间烧孔效应,实现了腔内横纵模协同调控,直接输出了单频矢量涡旋光束^[104]。面向小型化应用场景,本文作者团队报道了单块非平面环形腔(NPRO)涡旋激光器[图2(c)],将光纤激光器输出的泵浦光整形形成环形后泵浦单块Er:YAG NPRO,获得了1645 nm单频涡旋光束输出,激光线宽低至6 kHz^[105]。

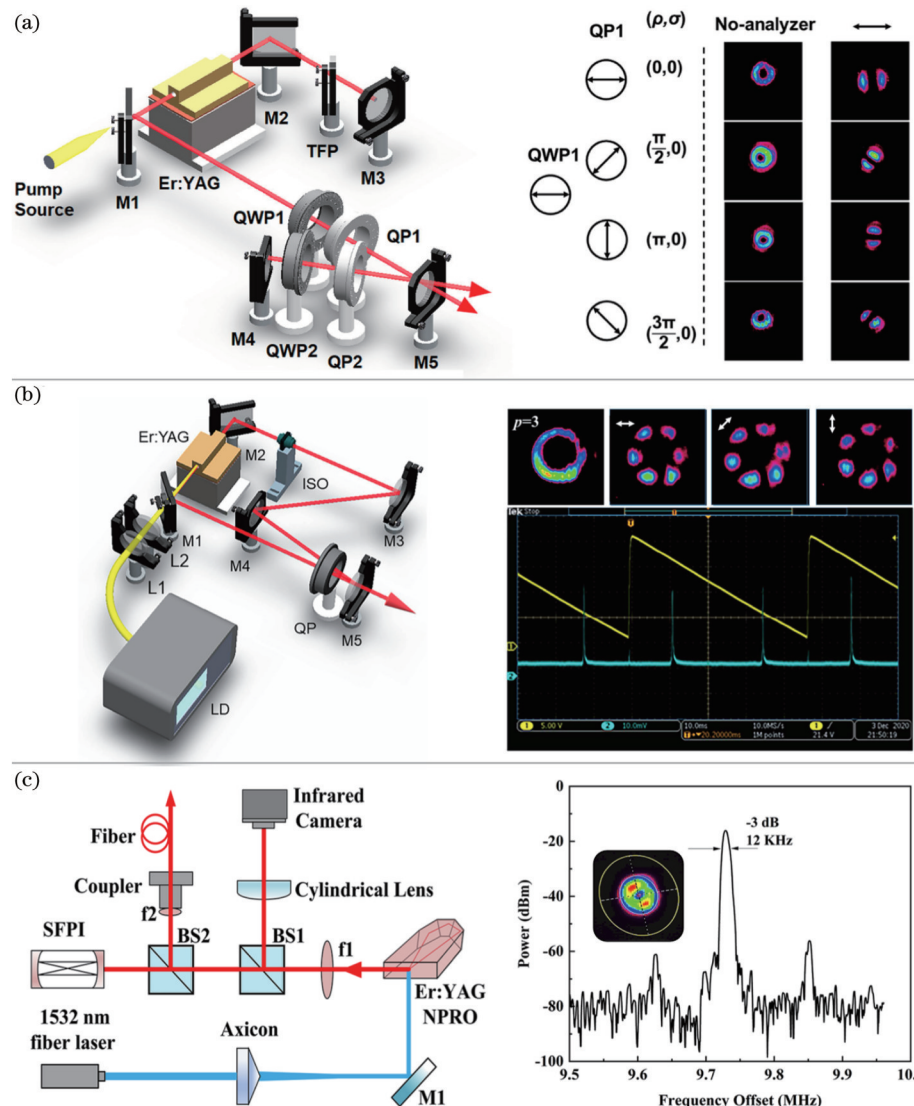


图2 本文作者团队研发的人眼安全矢量涡旋激光器。(a) V形腔结构矢量涡旋激光器^[103];(b) 环形腔单频矢量涡旋激光器^[104];(c) NPRO涡旋激光器^[105]

Fig. 2 Eye-safe vector vortex laser developed by our team. (a) V-shaped cavity vector vortex laser^[103]; (b) ring cavity vector vortex laser^[104]; (c) NPRO vortex laser^[105]

除上述给出的固体激光器外,采用光纤激光器^[106-109]及光学微腔^[110-116]等也可直接输出矢量涡旋光束,推动了矢量涡旋激光器技术小型化、集成化的进程。

4 矢量涡旋光束的模式识别方法

矢量涡旋光束的模式识别主要包括对其偏振分布的测量和对波前分布的测量,以此来表征其模场特征。最简单直观的偏振分布测量只需一个检偏器即可实现,将待测矢量涡旋光束通过检偏器,在不同的检偏器主轴角度下,出射光场的强度分布不同,以此反映其各向异性偏振特性,但该方案无法给出其全部模场特征。后来,研究人员提出了采用数字微镜阵列(DMD)等矢量涡旋光束的模场测量方案,将DMD编码特殊设计的振幅光栅配合光学系统,可定量测量待测矢量涡旋光束的杂合斯托克斯矢量分布^[117-119]。此外,还可采用液晶空间光调制器配合同轴干涉系统测量矢量涡旋光束的四参量表征^[52]。上述工作均提供了一种矢量涡旋光束的模场定量化测量方案。

矢量涡旋光束是对光场OAM和SAM协同调控的结果,在傍轴近似下,光子携带的总角动量(TAM)可表示为OAM和SAM的直积。这表明,如果能够精确地测量矢量涡旋光束的TAM分布,即可获得其模场特征。由于光子的SAM只有±1两个本征值,对应于宏观的左、右旋圆偏振态,因此对SAM分量的测量本质上就是对左、右旋圆偏振分量的测量,采用1/4波片配合检偏器即可实现。而光子的OAM具有无穷多个本征值,其对应宏观的螺旋波前分布,在测量上则相对复杂。综上,矢量涡旋光束的TAM分布测量的关键即在于OAM测量。国内外学者在光子OAM态测量及光束OAM谱识别方面开展了大量的研究工作,具体内容可参见本文作者团队之前发表的综述^[120-121],这里不再重复,而是重点介绍近三年本文作者团队在光束OAM分布测量方面的最新工作^[122-124]。

4.1 光束OAM谱的通用测量技术

本文作者团队于2020年报道了光束OAM谱的通用测量技术,其测量原理严格遵循光束OAM谱的定义,适用于任意光场分布的待测光束^[122]。光束OAM谱的定义式并不唯一,当前最常用的为基于光场螺旋谐波展开的定义。与傅里叶变换类似,光场的复振幅可以在螺旋谐波 $\exp(il\varphi)$ 下展开,表示为一系列螺旋谐波项 $\exp(il_k\varphi)$ 的累加形式,每个螺旋谐波项的复系数的模方即为OAM(功率)谱。为了严格遵循这一定义,需首先知悉待测光束的复振幅,复振幅包括振幅和相位两部分,振幅分布可通过面阵探测器直接测得,相位分布测量则较为复杂,因此测量光束的OAM谱本质上就是测量光束的相位分布。

图3(a)给出了本文作者团队提出的光束OAM谱测量的基本思路,即引入一参考高斯光束与待测光束

干涉,分别测量在有无 $\pi/2$ 延迟下的干涉场分布,以此来测量待测光束的相位,而后结合测得的待测光束振幅得到复振幅,再进行螺旋谐波展开运算,最终得到待测光束的OAM谱^[122]。采用该技术测量了包括多环涡旋光束在内的一系列复杂光场的OAM谱,实验结果与理论分析十分吻合。

4.2 深度学习辅助OAM谱测量技术

CCD、CMOS等面阵探测器的不断发展使得高分辨率测量光场强度分布成为可能,此外,深度学习作为涉及数学、计算机和生物等学科的强大工具,已经被成功而广泛地应用在医学图像处理、模式识别、图像分类等领域。这使得人们思考能否直接通过神经网络分析待测光束的强度分布,以此来准确、近乎实时地测量OAM谱。为了实现这一目标,本文作者团队根据OAM谱的特点,基于EfficientNet提出了Adjusted EfficientNet卷积神经网络结构,包含卷积层(其中滤波器尺寸为 3×3 或 1×1)、轻量反转瓶颈卷积层(滤波器尺寸为 3×3 或 5×5)、全局平均池化层以及一个全连接层,如图3(b)所示,以用于测量光束的OAM谱。实验过程中,采用一个特殊设计的相位光栅提取了待测光束的OAM特征,而后送至神经网络训练。共采集了27122组数据,其中24122组作为训练集,其余3000组作为验证集。训练好后的Adjusted EfficientNet神经网络可用于光束OAM谱测量。实验结果表明,同时存在7个不同OAM模式的情况下,OAM谱测量均方根误差低至 10^{-6} 数量级^[123]。

4.3 角向二次相位OAM分束器件

测量光束OAM谱的另一思路在于设法将待测光束中的不同OAM成分相互分离,而后根据分离开的模式间的相互位置关系确定待测光束的OAM分布。坐标变换法是当前较为成熟的OAM分束方法之一^[125-127],其核心在于将极坐标下的螺旋梯度相位转化为对数坐标下的横向倾斜相位,由于不同OAM模式对应的横向倾斜相位梯度不同,因此可经光场傅里叶变换相互分离。然而由于在坐标变换时引入了额外的像差,必须进行相位补偿,使得该方法必须采用双调制器件级联的结构。为了进一步简化OAM模式分束系统,本文作者团队设计了多环角向二次相位衍射器件,可将不同螺旋梯度下的OAM模式衍射至不同的角向空间位置^[124],如图3(c)所示。理论及实验研究表明,该方案在三环结构下,可支持最多73个OAM模式的同时分束,如果进一步优化相关参数(如增加相位环形结构数等),有望支持更多OAM模式。此外,基于该OAM模式分束器件,测量了光束的OAM谱,测量结果与理论值符合。

5 总 结

本文主要介绍了矢量涡旋光束的生成与模式识别方法,从矢量涡旋光束的基本原理、生成方法及模式识

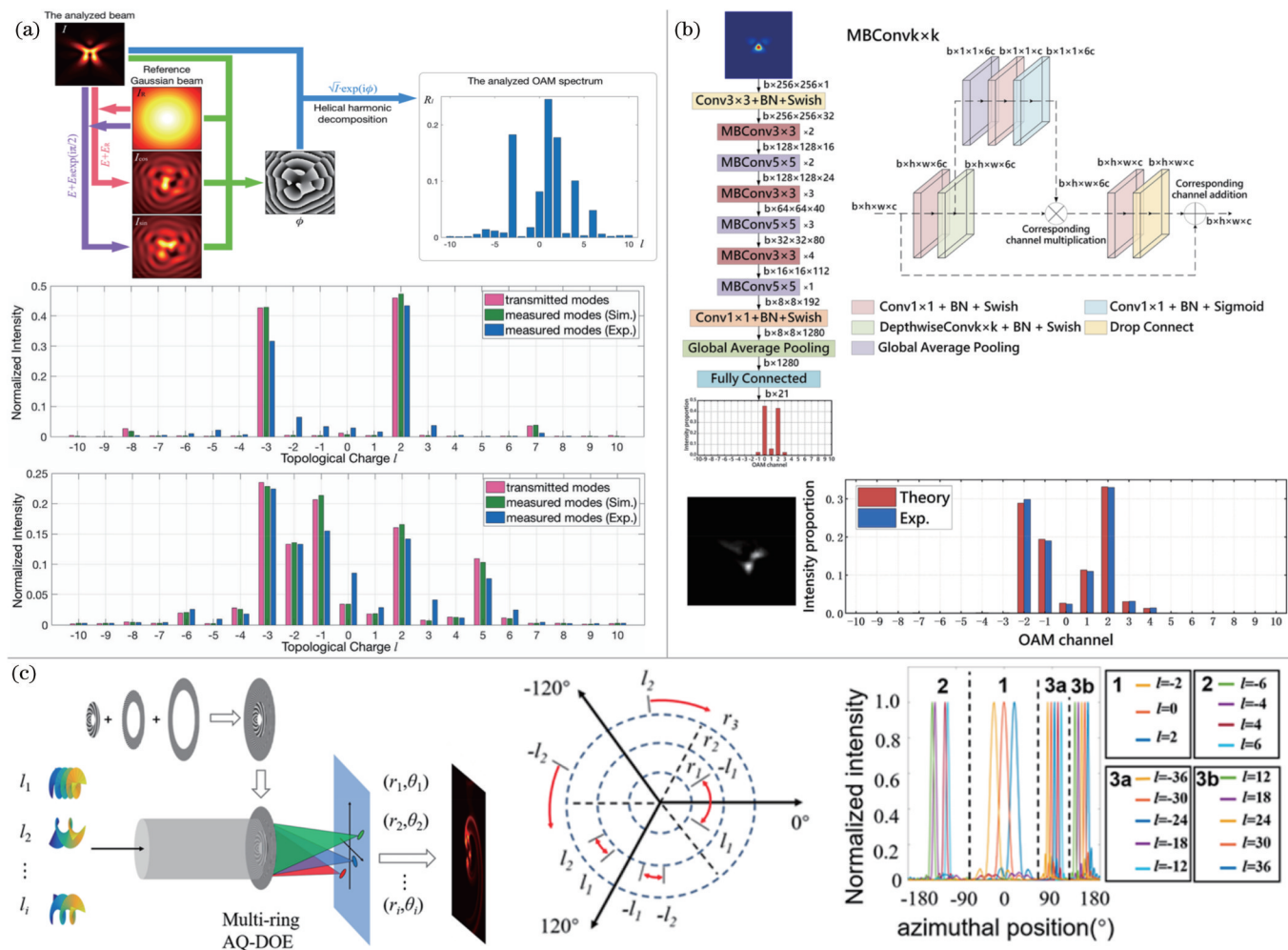


图3 本文作者团队研发的光束OAM模式测量技术。(a) 基于干涉的通用光束OAM谱测量^[122];(b) 深度学习辅助光束OAM谱测量^[123]; (c) 多环角向二次相位实现光束OAM分束^[124]

Fig. 3 Schemes of OAM mode measurement developed by our team. (a) Universal OAM spectra analyzer based on interference^[122]; (b) deep-learning assisted OAM spectrum measurement^[123]; (c) multi-ring azimuthal-quadratic phase enable OAM mode sorting^[124]

别方法三个方面回顾了国内外学者的主要工作。同时重点介绍了本文作者团队在该方面的代表性成果,包括矢量涡旋光束的四参量表征方法、腔外调控矢量涡旋光束光源、矢量涡旋光束激光器、光束OAM模式识别与分析处理等。尽管国内外学者已经在矢量涡旋光束的生成及模式识别方面开展了大量工作,但仍存在生成/模式识别系统不够小、支持模式动态范围不够广等局限,有待进一步突破。矢量涡旋光束的生成与模式识别是其应用的重要一环,随着相关理论与技术的不断成熟,面向未来系统化、融合化应用场景,小型化、紧凑化甚至芯片化将是未来矢量涡旋光束的生成与模式识别技术的发展方向之一。

参考文献

- [1] Poynting J H. The wave motion of a revolving shaft, and a suggestion as to the angular momentum in a beam of circularly polarised light[J]. Proceedings of the Royal Society A: Mathematical, Physical and Engineering Sciences, 1909, 82: 560-567.
- [2] Beth R A. Mechanical detection and measurement of the angular momentum of light[J]. Physical Review, 1936, 50(2): 115.
- [3] Jackson J D. Classical electrodynamics[M]. New York: Wiley, 1962.
- [4] Allen L, Beijersbergen M W, Spreeuw R J, et al. Orbital angular momentum of light and the transformation of Laguerre-Gaussian laser modes[J]. Physical Review A, Atomic, Molecular, and Optical Physics, 1992, 45(11): 8185-8189.
- [5] Yao A M, Padgett M J. Orbital angular momentum: origins, behavior and applications[J]. Advances in Optics and Photonics, 2011, 3(2): 161-204.
- [6] 高春清,付时尧. 涡旋光束[M]. 北京:清华大学出版社, 2019.
- [7] Zhan Q. Cylindrical vector beams: from mathematical concepts to applications[J]. Asian and Pacific Migration Journal: APMJ, 2009, 1(1): 1-57.
- [8] Forbes A, de Oliveira M, Dennis M R. Structured light[J]. Nature Photonics, 2021, 15(4): 253-262.
- [9] Wang J, Yang J Y, Fazal I M, et al. Terabit free-space data transmission employing orbital angular momentum multiplexing [J]. Nature Photonics, 2012, 6(7): 488-496.
- [10] Willner A E, Huang H, Yan Y, et al. Optical communications using orbital angular momentum beams[J]. Advances in Optics and Photonics, 2015, 7(1): 66-106.

- [11] Liu J Y, Zhang J X, Liu J, et al. 1-Pbps orbital angular momentum fibre-optic transmission[J]. *Light: Science & Applications*, 2022, 11(1): 1-11.
- [12] Fu S Y, Zhai Y W, Zhou H, et al. Demonstration of free-space one-to-many multicasting link from orbital angular momentum encoding[J]. *Optics Letters*, 2019, 44(19): 4753-4756.
- [13] Shang Z J, Fu S Y, Hai L, et al. Multiplexed vortex state array toward high-dimensional data multicasting[J]. *Optics Express*, 2022, 30(19): 34053-34063.
- [14] Lavery M P J, Speirs F C, Barnett S M, et al. Detection of a spinning object using lights orbital angular momentum[J]. *Science*, 2013, 341(6145): 537-540.
- [15] Fang L, Wan Z Y, Forbes A, et al. Vectorial Doppler metrology[J]. *Nature Communications*, 2021, 12(1): 1-10.
- [16] Guo H X, Qiu X D, Qiu S, et al. Frequency upconversion detection of rotational Doppler effect[J]. *Photonics Research*, 2022, 10(1): 183-188.
- [17] Fu S Y, Wang T L, Zhang Z Y, et al. Non-diffractive Bessel-Gauss beams for the detection of rotating object free of obstructions[J]. *Optics Express*, 2017, 25(17): 20098-20108.
- [18] Zhai Y W, Fu S Y, Yin C, et al. Detection of angular acceleration based on optical rotational Doppler effect[J]. *Optics Express*, 2019, 27(11): 15518-15527.
- [19] Padgett M, Bowman R. Tweezers with a twist[J]. *Nature Photonics*, 2011, 5(6): 343-348.
- [20] Yang Y J, Ren Y X, Chen M Z, et al. Optical trapping with structured light: a review[J]. *Advanced Photonics*, 2021, 3(3): 034001.
- [21] Fickler R, Lapkiewicz R, Huber M, et al. Interface between path and orbital angular momentum entanglement for high-dimensional photonic quantum information[J]. *Nature Communications*, 2014, 5(1): 1-6.
- [22] Cao H, Gao S C, Zhang C, et al. Distribution of high-dimensional orbital angular momentum entanglement a 1 km few-mode fiber [J]. *Optica*, 2020, 7(3): 232-237.
- [23] Li Z X, Zhu D, Lin P C, et al. High-dimensional entanglement generation based on a Pancharatnam-Berry phase metasurface[J]. *Photonics Research*, 2022, 10(12): 2702-2707.
- [24] Meier M, Romano V, Feurer T. Material processing with pulsed radially and azimuthally polarized laser radiation[J]. *Applied Physics A*, 2007, 86(3): 329-334.
- [25] Zheng J, Huang J X, Xu S L. Multiscale micro-/nanostructures on single crystalline SiC fabricated by hybridly polarized femtosecond laser[J]. *Optics and Lasers in Engineering*, 2020, 127: 105940.
- [26] Cui T, Sun L, Bai B, et al. Probing and imaging photonic spin-orbit interactions in nanostructures[J]. *Laser and Photonics Reviews*, 2021, 15(11): 2100011.
- [27] Bernet S, Jesacher A, Fürhapter S, et al. Quantitative imaging of complex samples by spiral phase contrast microscopy[J]. *Optics Express*, 2006, 14(9): 3792-3805.
- [28] Huang Y W, Rubin N A, Ambrosio A, et al. Versatile total angular momentum generation using cascaded J-plates[J]. *Optics Express*, 2019, 27(5): 7469-7484.
- [29] Liu S L, Liu S K, Yang C, et al. Classical simulation of high-dimensional entanglement by non-separable angular-radial modes [J]. *Optics Express*, 2019, 27(13): 18363-18375.
- [30] Liu S L, Zhou Q, Liu S K, et al. Classical analogy of a cat state using vortex light[J]. *Communications Physics*, 2019, 2(1): 1-9.
- [31] Wan Z S, Shen Y J, Liu Q, et al. Multipartite classically entangled scalar beams[J]. *Optics Letters*, 2022, 47(8): 2052-2055.
- [32] Shen Y J, Nape I, Yang X L, et al. Creation and control of high-dimensional multi-partite classically entangled light[J]. *Light: Science & Applications*, 2021, 10(1): 1-10.
- [33] Shen Y J, Rosales-Guzmán C. Nonseparable states of light: from quantum to classical[J]. *Laser & Photonics Reviews*, 2022, 16(7): 2100533.
- [34] Fu S Y, Shang Z J, Hai L, et al. Orbital angular momentum comb generation from azimuthal binary phases[J]. *Advanced Photonics Nexus*, 2022, 1(1): 016003.
- [35] Chong A, Wan C H, Chen J, et al. Generation of spatiotemporal optical vortices with controllable transverse orbital angular momentum[J]. *Nature Photonics*, 2020, 14(6): 350-354.
- [36] Wan C H, Chen J, Chong A, et al. Generation of ultrafast spatiotemporal wave packet embedded with time-varying orbital angular momentum[J]. *Science Bulletin*, 2020, 65(16): 1334-1336.
- [37] Cao Q, Chen J, Lu K Y, et al. Non-spreading Bessel spatiotemporal optical vortices[J]. *Science Bulletin*, 2022, 67(2): 133-140.
- [38] Wan C H, Cao Q, Chen J, et al. Toroidal vortices of light[J]. *Nature Photonics*, 2022, 16(7): 519-522.
- [39] Chen P, Ge S J, Duan W, et al. Digitalized geometric phases for parallel optical spin and orbital angular momentum encoding [J]. *ACS Photonics*, 2017, 4(6): 1333-1338.
- [40] Fu S Y, Zhang S K, Wang T L, et al. Rectilinear lattices of polarization vortices with various spatial polarization distributions [J]. *Optics Express*, 2016, 24(16): 18486-18491.
- [41] Fu S Y, Wang T L, Zhang Z Y, et al. Selective acquisition of multiple states on hybrid Poincaré sphere[J]. *Applied Physics Letters*, 2017, 110(19): 191102.
- [42] Rosales-Guzmán C, Bhebbe N, Forbes A. Simultaneous generation of multiple vector beams on a single SLM[J]. *Optics Express*, 2017, 25(21): 25697-25706.
- [43] Wang H, Fu S Y, Gao C Q. Tailoring a complex perfect optical vortex array with multiple selective degrees of freedom[J]. *Optics Express*, 2021, 29(7): 10811-10824.
- [44] Shen Y J, Yang X L, Naidoo D, et al. Structured ray-wave vector vortex beams in multiple degrees of freedom from a laser [J]. *Optica*, 2020, 7(7): 820-831.
- [45] Wang Z Y, Shen Y J, Naidoo D, et al. Astigmatic hybrid SU(2) vector vortex beams: towards versatile structures in longitudinally variant polarized optics[J]. *Optics Express*, 2021, 29(1): 315-329.
- [46] Shen Y J, Yang X L, Fu X, et al. Periodic-trajectory-controlled, coherent-state-phase-switched, and wavelength-tunable SU(2) geometric modes in a frequency-degenerate resonator[J]. *Applied Optics*, 2018, 57(32): 9543-9549.
- [47] Poincaré H. *Theorie mathematique de la Lumière*[M]. Paris: Gauthiers-Villars, 1892.
- [48] Milione G, Evans S, Nolan D A, et al. Higher order Pancharatnam-Berry phase and the angular momentum of light [J]. *Physical Review Letters*, 2012, 108(19): 190401.
- [49] Milione G, Sztul H I, Nolan D A, et al. Higher-order Poincaré sphere, stokes parameters, and the angular momentum of light [J]. *Physical Review Letters*, 2011, 107(5): 053601.
- [50] Yi X N, Liu Y C, Ling X H, et al. Hybrid-order Poincaré sphere[J]. *Physical Review A*, 2015, 91(2): 023801.
- [51] Ren Z C, Rong L J, Li S M, et al. Generalized Poincaré sphere [J]. *Optics Express*, 2015, 23(20): 26586-26595.
- [52] Fu S Y, Hai L, Song R, et al. Representation of total angular momentum states of beams through a four-parameter notation[J]. *New Journal of Physics*, 2021, 23(8): 083015.
- [53] Jones P H, Rashid M, Makita M, et al. Sagnac interferometer method for synthesis of fractional polarization vortices[J]. *Optics Letters*, 2009, 34(17): 2560-2562.
- [54] Liu S, Li P, Peng T, et al. Generation of arbitrary spatially variant polarization beams with a trapezoid Sagnac interferometer [J]. *Optics Express*, 2012, 20(19): 21715-21721.
- [55] Li P, Zhang Y, Liu S, et al. Generation of perfect vectorial vortex beams[J]. *Optics Letters*, 2016, 41(10): 2205-2208.
- [56] Wang X L, Ding J P, Ni W J, et al. Generation of arbitrary

- vector beams with a spatial light modulator and a common path interferometric arrangement[J]. *Optics Letters*, 2007, 32(24): 3549-3551.
- [57] Liu S, Qi S X, Zhang Y, et al. Highly efficient generation of arbitrary vector beams with tunable polarization, phase, and amplitude[J]. *Photonics Research*, 2018, 6(4): 228-233.
- [58] Fu S Y, Gao C Q, Shi Y, et al. Generating polarization vortices by using helical beams and a Twyman Green interferometer[J]. *Optics Letters*, 2015, 40(8): 1775-1778.
- [59] Wang T L, Fu S Y, Zhang S K, et al. A Sagnac-like interferometer for the generation of vector beams[J]. *Applied Physics B*, 2016, 122(9): 231.
- [60] Wang T L, Fu S Y, He F, et al. Generation of perfect polarization vortices using combined gratings in a single spatial light modulator[J]. *Applied Optics*, 2017, 56(27): 7567-7571.
- [61] Xin J T, Gao C Q, Li C, et al. Generation of polarization vortices with a Wollaston prism and an interferometric arrangement[J]. *Applied Optics*, 2012, 51(29): 7094-7097.
- [62] Fu S Y, Zhai Y W, Wang T L, et al. Tailoring arbitrary hybrid Poincaré beams through a single hologram[J]. *Applied Physics Letters*, 2017, 111(21): 211101.
- [63] Moreno I, Davis J A, Hernandez T M, et al. Complete polarization control of light from a liquid crystal spatial light modulator[J]. *Optics Express*, 2012, 20(1): 364-376.
- [64] Moreno I, Davis J A, Cottrell D M, et al. Encoding high-order cylindrically polarized light beams[J]. *Applied Optics*, 2014, 53(24): 5493-5501.
- [65] Han W, Yang Y F, Cheng W, et al. Vectorial optical field generator for the creation of arbitrarily complex fields[J]. *Optics Express*, 2013, 21(18): 20692-20706.
- [66] Cai M Q, Wang Z X, Liang J, et al. High-efficiency and flexible generation of vector vortex optical fields by a reflective phase-only spatial light modulator[J]. *Applied Optics*, 2017, 56(22): 6175-6180.
- [67] Fu S Y, Wang T L, Gao C Q. Generating perfect polarization vortices through encoding liquid-crystal display devices[J]. *Applied Optics*, 2016, 55(23): 6501-6505.
- [68] Fu S Y, Gao C Q, Wang T L, et al. Simultaneous generation of multiple perfect polarization vortices with selective spatial states in various diffraction orders[J]. *Optics Letters*, 2016, 41(23): 5454-5457.
- [69] Fu S Y, Gao C Q, Wang T L, et al. Anisotropic polarization modulation for the production of arbitrary Poincaré beams[J]. *Journal of the Optical Society of America B*, 2018, 35(1): 1-7.
- [70] Zhou H, Gao C Q, Fu S Y, et al. Experimental demonstration of generating arbitrary total angular momentum states[J]. *Chinese Optics Letters*, 2020, 18(11): 110503.
- [71] Passilly N, de Saint Denis R, Ait-Ameur K, et al. Simple interferometric technique for generation of a radially polarized light beam[J]. *Journal of the Optical Society of America A: Optics, Image Science, and Vision*, 2005, 22(5): 984-991.
- [72] Phua P B, Lai W J. Simple coherent polarization manipulation scheme for generating high power radially polarized beam[J]. *Optics Express*, 2007, 15(21): 14251-14256.
- [73] Bashkansky M, Park D, Fatemi F K. Azimuthally and radially polarized light with a nematic SLM[J]. *Optics Express*, 2010, 18(1): 212-217.
- [74] Bliokh K Y, Rodríguez-Fortuño F J, Nori F, et al. Spin - orbit interactions of light[J]. *Nature Photonics*, 2015, 9(12): 796-808.
- [75] Liu Y C, Ke Y G, Luo H L, et al. Photonic spin Hall effect in metasurfaces: a brief review[J]. *Nanophotonics*, 2016, 6(1): 51-70.
- [76] Chen P, Wei B Y, Hu W, et al. Liquid-crystal-mediated geometric phase: from transmissive to broadband reflective planar optics[J]. *Advanced Materials*, 2020, 32(27): 1903665.
- [77] Marrucci L, Manzo C, Paparo D. Optical spin-to-orbital angular momentum conversion in inhomogeneous anisotropic media[J]. *Physical Review Letters*, 2006, 96(16): 163905.
- [78] Liu Z X, Liu Y Y, Ke Y G, et al. Generation of arbitrary vector vortex beams on hybrid-order Poincaré sphere[J]. *Photonics Research*, 2017, 5(1): 15-21.
- [79] Xin J T, Dai K J, Zhong L, et al. Generation of optical vortices by using spiral phase plates made of polarization dependent devices[J]. *Optics Letters*, 2014, 39(7): 1984-1987.
- [80] Yu N F, Genevet P, Kats M A, et al. Light propagation with phase discontinuities: generalized laws of reflection and refraction [J]. *Science*, 2011, 334(6054): 333-337.
- [81] Kim J, Seong J, Yang Y, et al. Tunable metasurfaces towards versatile metaleenses and metaholograms: a review[J]. *Advanced Photonics*, 2022, 4(2): 024001.
- [82] Hsiao H H, Chu C H, Tsai D P. Fundamentals and applications of metasurfaces[J]. *Small Methods*, 2017, 1(4): 1600064.
- [83] Wang X W, Nie Z Q, Liang Y, et al. Recent advances on optical vortex generation[J]. *Nanophotonics*, 2018, 7(9): 1533-1556.
- [84] Yue F Y, Wen D D, Zhang C M, et al. Multichannel polarization-controllable superpositions of orbital angular momentum states[J]. *Advanced Materials*, 2017, 29(15): 1603838.
- [85] Zhang X, Huang L L, Zhao R Z, et al. Multiplexed generation of generalized vortex beams with on-demand intensity profiles based on metasurfaces[J]. *Laser & Photonics Reviews*, 2022, 16(3): 2100451.
- [86] Zhou H, Yang J Q, Gao C Q, et al. High-efficiency, broadband all-dielectric transmission metasurface for optical vortex generation[J]. *Optical Materials Express*, 2019, 9(6): 2699.
- [87] Zhang Z C, Hai L, Fu S Y, et al. Advances on solid-state vortex laser[J]. *Photonics*, 2022, 9(4): 215.
- [88] Kim D J, Kim J W. Direct generation of an optical vortex beam in a single-frequency Nd: YVO₄ laser[J]. *Optics Letters*, 2015, 40(3): 399-402.
- [89] Yao Y, Xia K G, Kang M Q, et al. Transverse mode transition and LG01-mode generation in an end-pumped Nd: YVO₄ laser [J]. *Chinese Optics Letters*, 2013, 11(12): 121406.
- [90] Oh Y J, Kim T H, Park E J, et al. Direct generation of the first-radial-order Laguerre - Gaussian mode in a Nd: YVO₄ laser incorporating a core-ring-shaped pump fibre[J]. *Laser Physics*, 2020, 30(9): 095801.
- [91] He H S, Chen Z, Li H B, et al. Low-threshold, nanosecond, high-repetition-rate vortex pulses with controllable helicity generated in Cr, Nd: YAG self-Q-switched microchip laser[J]. *Laser Physics*, 2018, 28(5): 055802.
- [92] Chen D M, Miao Y J, Fu H, et al. High-order cylindrical vector beams with tunable topological charge up to 14 directly generated from a microchip laser with high beam quality and high efficiency[J]. *APL Photonics*, 2019, 4(10): 106106.
- [93] Ding Y S, Yang J W, Chen D M, et al. Rectangular beam pumped Raman microchip laser for generating multiwavelength high-order Hermite - Gaussian lasers and vortex lasers[J]. *Annalen Der Physik*, 2022, 534(6): 2200095.
- [94] Li K, Tang K F, Lin D, et al. Direct generation of optical vortex beams with tunable topological charges up to 18th using an axicon[J]. *Optics & Laser Technology*, 2021, 143: 107339.
- [95] Lin G P, Cao Y Q, Ji R R, et al. Direct generation of a narrow-linewidth Laguerre - Gaussian vortex laser in a monolithic nonplanar oscillator[J]. *Optics Letters*, 2018, 43(17): 4164-4167.
- [96] Qiao Z, Xie G Q, Wu Y H, et al. Generating high-charge optical vortices directly from laser up to 288th order[J]. *Laser & Photonics Reviews*, 2018, 12(8): 1800019.
- [97] Qiao Z, Wan Z Y, Xie G, et al. Multi-vortex laser enabling spatial and temporal encoding[J]. *PhotoniX*, 2020, 1: 1-14.
- [98] Ngcobo S, Litvin I, Burger L, et al. A digital laser for on-demand laser modes[J]. *Nature Communications*, 2013, 4(1): 1-6.

- [99] Naidoo D, Roux F S, Dudley A, et al. Controlled generation of higher-order Poincaré sphere beams from a laser[J]. *Nature Photonics*, 2016, 10(5): 327-332.
- [100] Sroor H, Huang Y W, Sephton B, et al. High-purity orbital angular momentum states from a visible metasurface laser [J]. *Nature Photonics*, 2020, 14(8): 498-503.
- [101] Piccardo M, de Oliveira M, Toma A, et al. Vortex laser arrays with topological charge control and self-healing of defects[J]. *Nature Photonics*, 2022, 16: 359-365.
- [102] Sheng Q, Wang A H, Ma Y Y, et al. Intracavity spherical aberration for selective generation of single-transverse-mode Laguerre-Gaussian output with order up to 95[J]. *Photonix*, 2022, 3(1): 1-12.
- [103] Song R, Gao C Q, Zhou H, et al. Resonantly pumped Er: YAG vector laser with selective polarization states at 1.6 μm [J]. *Optics Letters*, 2020, 45(16): 4626-4629.
- [104] Song R, Liu X T, Fu S Y, et al. Simultaneous tailoring of longitudinal and transverse mode inside an Er: YAG laser[J]. *Chinese Optics Letters*, 2021, 19(11): 111404.
- [105] Wang K X, Zhang X, Fu S Y, et al. 1645-nm single-frequency vortex laser from an Er: YAG nonplanar ring oscillator[J]. *Optics Letters*, 2023, 48(2): 331-334.
- [106] Liu J, Chen S, Wang H Y, et al. Amplifying orbital angular momentum modes in ring-core erbium-doped fiber[J]. *Research*, 2020, 2020: 7623751.
- [107] Jiang X H, Yao J N, Zhang S Y, et al. All-fiber switchable orbital angular momentum mode-locked laser based on TM-FBG [J]. *Applied Physics Letters*, 2022, 121(13): 131101.
- [108] Wang S Q, Li Y, Zhao S, et al. Switchable transverse mode operation of a fiber laser with an external feedback cavity[J]. *Laser Physics Letters*, 2021, 18(10): 105101.
- [109] Ji K H, Lin D, Davidson I A, et al. Controlled generation of picosecond-pulsed higher-order Poincaré sphere beams from an ytterbium-doped multicore fiber amplifier[J]. *Photonics Research*, 2022, 11(2): 181-188.
- [110] Cai X L, Wang J W, Strain M, et al. Integrated compact optical vortex beam emitters[J]. *Science*, 2012, 338(6105): 363-366.
- [111] Li S M, Ding Y H, Guan X W, et al. Compact high-efficiency vortex beam emitter based on a silicon photonics micro-ring[J]. *Optics Letters*, 2018, 43(6): 1319-1322.
- [112] Zhang J, Sun C Z, Xiong B, et al. An InP-based vortex beam emitter with monolithically integrated laser[J]. *Nature Communications*, 2018, 9(1): 1-6.
- [113] Xie Z W, Lei T, Li F, et al. Ultra-broadband on-chip twisted light emitter for optical communications[J]. *Light: Science & Applications*, 2018, 7(4): 18001.
- [114] Liu Y W, Lao C H, Wang M, et al. Integrated vortex soliton microcombs[EB/OL]. (2022-12-15)[2023-01-05]. <https://arxiv.org/abs/2212.07639>.
- [115] Wang Y, Zhao P, Feng X, et al. Integrated photonic emitter with a wide switching range of orbital angular momentum modes [J]. *Scientific Reports*, 2016, 6(1): 1-9.
- [116] Zhang Q, Ni J C, Qiu C W. Vortex 4.0 on chip[J]. *Light, Science & Applications*, 2020, 9: 103.
- [117] Hu X B, Guzman C R. Generation and characterization of complex vector modes with digital micromirror devices: a tutorial [J]. *Journal of Optics*, 2022, 24:034001.
- [118] Zhao B, Hu X B, Rodríguez-Fajardo V, et al. Determining the non-separability of vector modes with digital micromirror devices [J]. *Applied Physics Letters*, 2020, 116(9): 091101.
- [119] Zhao B, Hu X B, Rodríguez-Fajardo V, et al. Real-time Stokes polarimetry using a digital micromirror device[J]. *Optics Express*, 2019, 27(21): 31087-31093.
- [120] 付时尧, 高春清. 利用衍射光栅探测涡旋光束轨道角动量态的研究进展[J]. *物理学报*, 2018, 67(3): 034201.
- Fu S Y, Gao C Q. Progress of detecting orbital angular momentum states of optical vortices through diffraction gratings [J]. *Acta Physica Sinica*, 2018, 67(3): 034201.
- [121] 付时尧, 黄磊, 吕燕来, 等. 光束轨道角动量谱的测量技术研究进展(特邀)[J]. *红外与激光工程*, 2021, 50(9): 20210145.
- Fu S Y, Huang L, Lü Y L, et al. Advances on the measurement of orbital angular momentum spectra for laser beams(Invited)[J]. *Infrared and Laser Engineering*, 2021, 50(9): 20210145.
- [122] Fu S, Zhai Y, Zhang J, et al. Universal orbital angular momentum spectrum analyzer for beams [J]. *Photonix*, 2020, 1 (1): 19.
- [123] Wang J Q, Fu S Y, Shang Z J, et al. Adjusted EfficientNet for the diagnostic of orbital angular momentum spectrum[J]. *Optics Letters*, 2022, 47(6): 1419-1422.
- [124] Lü Y L, Shang Z J, Fu S Y, et al. Sorting orbital angular momentum of photons through a multi-ring azimuthal-quadratic phase[J]. *Optics Letters*, 2022, 47(19): 5032-5035.
- [125] Berkhout G C G, Lavery M P J, Courtial J, et al. Efficient sorting of orbital angular momentum states of light[J]. *Physical Review Letters*, 2010, 105(15): 153601.
- [126] Mirhosseini M, Malik M, Shi Z M, et al. Efficient separation of the orbital angular momentum eigenstates of light[J]. *Nature Communications*, 2013, 4: 2781.
- [127] Wen Y H, Chremmos I, Chen Y J, et al. Spiral transformation for high-resolution and efficient sorting of optical vortex modes [J]. *Physical Review Letters*, 2018, 120(19): 193904.

Generation and Mode Recognition Method of Vectorial Vortex Beams

Fu Shiyao^{1,2,3*}, Gao Chunqing^{1,2,3**}

¹School of Optics and Photonics, Beijing Institute of Technology, Beijing 100081, China;

²Key Laboratory of Information Photonics Technology, Ministry of Industry and Information Technology, Beijing 100081, China;

³Key Laboratory of Photoelectronic Imaging Technology and System, Ministry of Education, Beijing 100081, China

Abstract

Significance Similar to macroscopic objects, photons can also carry angular momentum, such as spin angular momentum (SAM) and orbital angular momentum (OAM). The two angular momenta contribute to a new structured beam, the

vectorial vortex beam (VVB). A VVB has anisotropic wavefront and polarization distributions, thus providing multiple degrees of freedom and showing great potential in lots of advanced domains including quantum technology, laser communications, laser detection, laser processing, high-resolution imaging, and optical tweezers, attracting much attention around the world. The key to employing VVBs in these above scenarios is their generation and recognition with high performance. We review recent advances in generating and diagnosing VVBs in brief. In addition, we also systematically review research on this topic from our team in the past decade and focus more on our representative achievements.

Progress This review consists of three main sections. The basic principles of VVBs are introduced in the first section. The introduction begins with the decomposition of VVBs, as a VVB can be regarded as the coaxial superposition of two scalar beams with opposite SAM and various OAMs. Then, typical representations of VVBs, the hybrid order Stokes parameters, and Poincare spheres are reviewed. Finally, our recent demonstration for VVB mode representation, the four-parameter notation, and its great performance is introduced.

The second section presents recent advances in VVB generation, including extra- and intra- cavity generations. The extra-cavity generation scheme is to transform other beams containing Gaussian beams and Hermit-Gauss beams into VVBs outside a laser resonator, whose principle is based on the decomposition of VVBs. In addition, such a scheme is flexible to produce more complex vectorial vortex fields, including the VVB array and perfect vortex array. By employing programmable devices of the liquid-crystal spatial light modulator, VVBs can also be generated digitally. The intra-cavity generation scheme is to output VVBs from a laser resonator directly. One can place multiple devices or optical elements inside the cavity, thereby leading to the oscillation of high-order transverse modes including VVBs. One of the most common intra-cavity elements is Q-plate, with photon SAM-OAM conversion elements fabricated based on photon spin Hall effect. Such elements can transform the oscillated fundamental mode to vectorial vortex mode and meet with the mode self-consistence in a laser cavity. Furthermore, the spatial light modulator can also be employed as part of the resonator to replace the end mirror to form a "digital laser" and enable VVBs output. Our recent work is also presented emphatically in this section, including eye-safe solid VVB lasers, single frequency VVB lasers, and nonplanar ring oscillator VVB lasers.

The third section presents recent advances in the vectorial vortex mode recognition. Vectorial vortex mode originates from the classical entanglement of SAM and OAM. Thus a VVB is also a total angular momentum (TAM) mode, and vectorial vortex mode recognition is equivalent to TAM measurement. As photon SAM has only two eigenvalues, the key to vectorial vortex mode recognition is to measure OAM distribution. This section introduces more about OAM analysis developed by our team, including universal OAM spectrum analyzer, deep learning-assisted OAM spectrum measurement, and photon OAM sorter. The universal OAM spectrum analyzer is based on the helical harmonic decomposition of beams, which is the definition of the OAM spectrum. Therefore, such an analyzer is universal and appropriate for beams with any patterns. The deep learning-assisted OAM spectrum measurement is to extract OAM features firstly and analyze the extracted pattern through our developed convolutional neural network, the adjusted EfficientNet. The OAM sorter is accomplished through our developed multi-ring azimuthal-quadratic phase, and supports up to 73 OAM modes.

Prospects We hope this review will provide more useful information for people who study VVBs and their applications, and inspire more novel and wonderful ideas.

Key words physical optics; laser field manipulation; vectorial vortex beam; orbital angular momentum; spin angular momentum